

# RSC Pharmaceutics

Accepted Manuscript

This article can be cited before page numbers have been issued, to do this please use: G. Choudhary, S. Jadoun, K. Rani, A. Sharma and M. Lakavathu, *RSC Pharm.*, 2026, DOI: 10.1039/D6PM00077K.



This is an Accepted Manuscript, which has been through the Royal Society of Chemistry peer review process and has been accepted for publication.

Accepted Manuscripts are published online shortly after acceptance, before technical editing, formatting and proof reading. Using this free service, authors can make their results available to the community, in citable form, before we publish the edited article. We will replace this Accepted Manuscript with the edited and formatted Advance Article as soon as it is available.

You can find more information about Accepted Manuscripts in the [Information for Authors](#).

Please note that technical editing may introduce minor changes to the text and/or graphics, which may alter content. The journal's standard [Terms & Conditions](#) and the [Ethical guidelines](#) still apply. In no event shall the Royal Society of Chemistry be held responsible for any errors or omissions in this Accepted Manuscript or any consequences arising from the use of any information it contains.

## ARTICLE

# Dual Cross-linked Biodegradable Polyelectrolyte Hydrogel Actuator for Bi-Directional pH-Responsive Drug Release

Govind Choudhary<sup>1</sup>, Soni Jadoun<sup>1</sup>, Komal Rani<sup>1</sup>, Manikrishna Lakavathu<sup>2</sup>, Aashish Sharma<sup>1\*</sup>Received 00th January 20xx,  
Accepted 00th January 20xx

DOI: 10.1039/x0xx00000x

**Abstract:**

Here, we present a dual cross-linked pH-responsive hydrogel platform for controlled drug release in acidic as well as basic pathophysiological pH media. The hydrogel was strategically developed using oppositely charged polyelectrolytes, namely gelatin and carboxymethyl cellulose (CMC). This hydrogel was stabilised by adding a cross-linking agent, 1,4-butanediol diglycidyl ether (BDDE). The hydrogel could be formulated in about 2 hr, at pH 9, without any specialised instruments. The prepared hydrogel senses both lower and higher environmental pH and swells to deliver the drug to the intended application site. Importantly, the prepared hydrogel was found to exhibit equal percentage (~60%) of shrinkage (at 7.4) and swelling (at pH 4 and 9). The novelty of the proposed hydrogel lies in its reversible sensitivity to pH for on-demand drug delivery both in acidic environments (e.g. tumour site) and basic environments (e.g. chronic wounds). Neomycin sulphate, a common drug effective against chronic wounds and cancer, could be entrapped within the hydrogel with excellent entrapment efficiency (~84%). Entrapped neomycin sulphate is released on-demand in acidic (pH~6) as well as basic (pH~9) medium. This polyelectrolyte-based hydrogel gets bio-degraded within 21 days. Changes in the hydrogel's morphology were observed through SEM. The reported hydrogel exhibits remarkable biocompatibility also for HeLa cell lines. Therefore, this prepared hydrogel may be a promising pH-responsive biomaterial for drug delivery applications, which can easily be scaled up in future.

## 1. Introduction

In recent years, hydrogels have drawn the interest of biomaterials scientists as one of the most promising drug delivery technologies for various modes of administration, including topical, parenteral, oral, ocular, vaginal and rectal.<sup>1–3</sup> Because of their exceptionally high water content, hydrogels exhibit excellent biocompatibility, have a morphological resemblance to human tissues, and have a tunable capacity to encapsulate hydrophilic drugs.<sup>3</sup> These encapsulated drugs can be released from hydrogels in response to certain stimuli like pH, temperature, enzymes, certain biomolecules (e.g. glucose) and reactive oxygen species.<sup>4–6</sup> These stimuli-responsive hydrogels integrate controlled drug delivery due to their ability to respond to the above-mentioned external stimuli. Such stimuli-responsive hydrogels incorporate various polymers and cross-linkers according to the intended stimuli. Among all the above-mentioned stimuli, tissue-specific pH in healthy and diseased conditions is being highly explored to develop stimuli-responsive hydrogels for drug delivery applications. For example, lower pH in the vicinity of cancer cells and

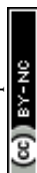
higher pH of chronic wounds as compared to the physiological pH have been utilised for drug delivery purposes.<sup>7,8</sup> pH-responsive hydrogels have also been reported to deliver the drugs in various conditions like peptic ulcer, respiratory diseases, ulcerative colitis, arthritis, bacterial infections, etc.<sup>2,9</sup> But the majority of the reported pH-sensitive hydrogels sense either acidic or basic pH only, hence can deliver the encapsulated drug in the pathological conditions resulting in either acidic or basic pH medium. The current exploration endeavoured to resolve this problem by meticulous selection of ionizable polymers (polyelectrolytes).

For addressing this problem, we reviewed numerous reports about pH-responsive hydrogels and found that the reported hydrogels incorporate various natural and synthetic polymers bearing pH-dependent cationic charge (cationic polyelectrolytes) and anionic charge (anionic polyelectrolytes).<sup>10,11</sup> Mainly; chitosan<sup>12,13</sup>, gelatin<sup>14–16</sup>, collagen<sup>17,18</sup>, PEI<sup>19,20</sup>, poly(amino)methacrylate/poly(amino) acrylate<sup>21</sup>, poly( $\beta$ -aminoester)<sup>21</sup>, polyurethane<sup>21</sup>, poly(4-vinylpyridine)<sup>22</sup>, are used as cationic polyelectrolytes, while alginate<sup>9,23</sup>, hyaluronic acid<sup>24,25</sup>, chondroitin sulphate<sup>26</sup>, carboxymethyl cellulose<sup>27,28</sup>, carrageenan<sup>29</sup>, polyaspartic acid<sup>30,31</sup>, polyacrylic acid<sup>32,33</sup> etc. are used as anionic polyelectrolytes to formulate pH-responsive hydrogels. These polyelectrolytes interact through electrostatic interactions to create a 3D network of hydrogel, which holds water and can entrap various

<sup>1</sup>Address: Department of Pharmacy, School of Healthcare and Allied Sciences, Sohna- Gurugram Road, Sohna-122103, Gurugram, Haryana, India.

<sup>2</sup>Indian Institute of Science Education and Research Thiruvananthapuram (IISER TVM), Maruthamala, PO, Vithura, Thiruvananthapuram - 695551. Kerala, India.

\*Email: pharma.aashish@gmail.com



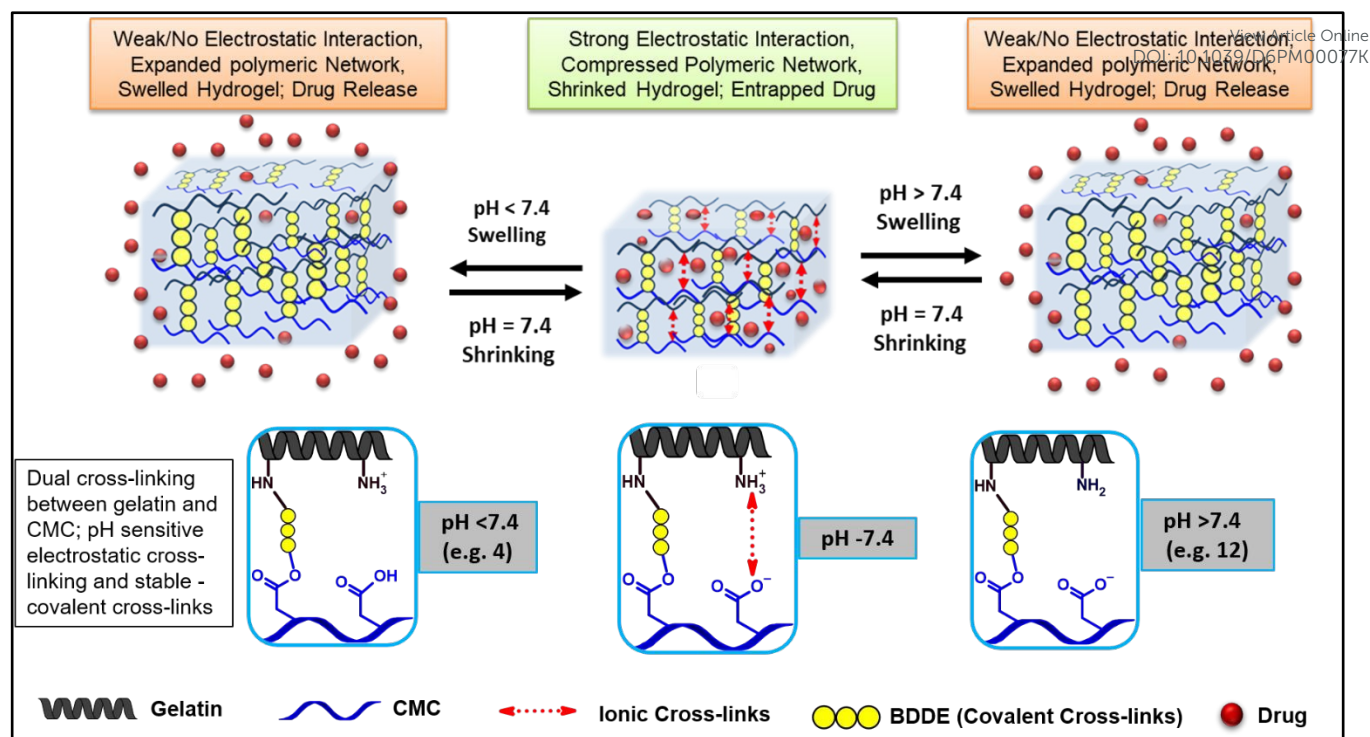


**Figure 1:** Showcasing the basic design of bi-directional pH-sensitive hydrogel, pH-responsive drug release and dual cross-linking between gelatin and CMC.

drugs. These electrostatic interactions are pH dependent; hence make the hydrogel unstable beyond a certain pH range. Changing the pH beyond a particular value may neutralise the charge on these polyelectrolytes and allow both of the counter polyelectrolytes to separate from each other. The separation of neutralised polyelectrolytes of a hydrogel becomes more prominent when hydrogels soak an aqueous medium. During the process of soaking, the inflow of water molecules into the hydrogels expels the neutralised polyelectrolytes forcefully apart from each other, resulting in swelling of the hydrogels, which in turn makes the hydrogels highly unstable. In this process, the entrapped drug gets released from such hydrogels without any control (viz., burst release).<sup>10</sup>

This uncontrolled drug release resulted from the complete separation of neutral polyelectrolytes of hydrogels. Here, we endeavoured to hinder the separation of neutralised polyelectrolytes for controlling the burst release by putting suitable covalent cross-links between the counter polyelectrolytes. These covalent cross-links keep holding both of the polyelectrolytes even in the charge-neutralised condition during swelling of the hydrogels. These covalent cross-links act as anchors that allow neutralised polyelectrolytes to move upon swelling but prevent complete disruption of the hydrogels to control the drug release as a function of pH.<sup>3</sup>

Researchers have employed various cross-linking chemistries for developing hydrogels, which mainly include Schiff's base,<sup>34–36</sup> disulphide bonds,<sup>37,38</sup> thiol-ene,<sup>39–41</sup> thiol-yne,<sup>41,42</sup> alkyne-azide,<sup>43</sup> thiol-michael addition,<sup>44</sup> DOPA crosslinks,<sup>45</sup> and enzymatic cross-

linking<sup>46–48</sup> to name a few. For employing these cross-linking chemistries, either natural polymers are derivatised with suitable functionalities or entirely new polymers have to be synthesised. Sometimes, functionalization of natural polymers is a prerequisite condition for employing different cross-linking chemistries, which may bring these polymers out of the FDA-approved list. However, incorporating FDA-approved polymers in hydrogels may enhance the chances of commercialisation of such formulations.<sup>49</sup>

Moreover, some of the cross-linking chemistries additionally need external impetus, such as thiol-ene/thiol-yne cross-linking, which requires photo-initiators and UV-light.<sup>39–41</sup> Alkyne-azide cross-links need a copper-based catalyst,<sup>43</sup> thiol-maleimide chemistry needs a suitable base,<sup>50</sup> DOPA-based cross-links entail either metal ion ( $\text{Fe}^{+3}$ ) or periodates or enzymes,<sup>51–53</sup> while enzymatic cross-links unequivocally need suitable enzymes to cross-link the polyelectrolytes.<sup>54,55</sup> Although few reported thiolated polyelectrolytes can form disulphide bonds (thiol-to disulphide conversions) without any external reagent, this has been explored by us in our earlier published reports.<sup>56,57</sup>

Apart from the above-mentioned cross-linkers, there are certain cross-linkers such as glutaraldehyde, 1,4-butanediol diglycidyl ether (BDDE), divinyl sulphone (DVS), etc., which can cross-link the different biopolymers without further functionalization.<sup>58–60</sup> Glutaraldehyde (GTA) (including other dialdehyde analogues), BDDE and DVS can crosslink chitosan,<sup>61–63</sup> gelatin,<sup>58,64,65</sup> collagen<sup>66–68</sup> through their amine functionalities. Anionic polymers such as hyaluronic acid,<sup>69</sup> carboxymethyl cellulose,<sup>70–72</sup> starch<sup>73</sup>, etc., have also been cross-linked successfully for developing different biomaterial formulations. Most of the researchers used



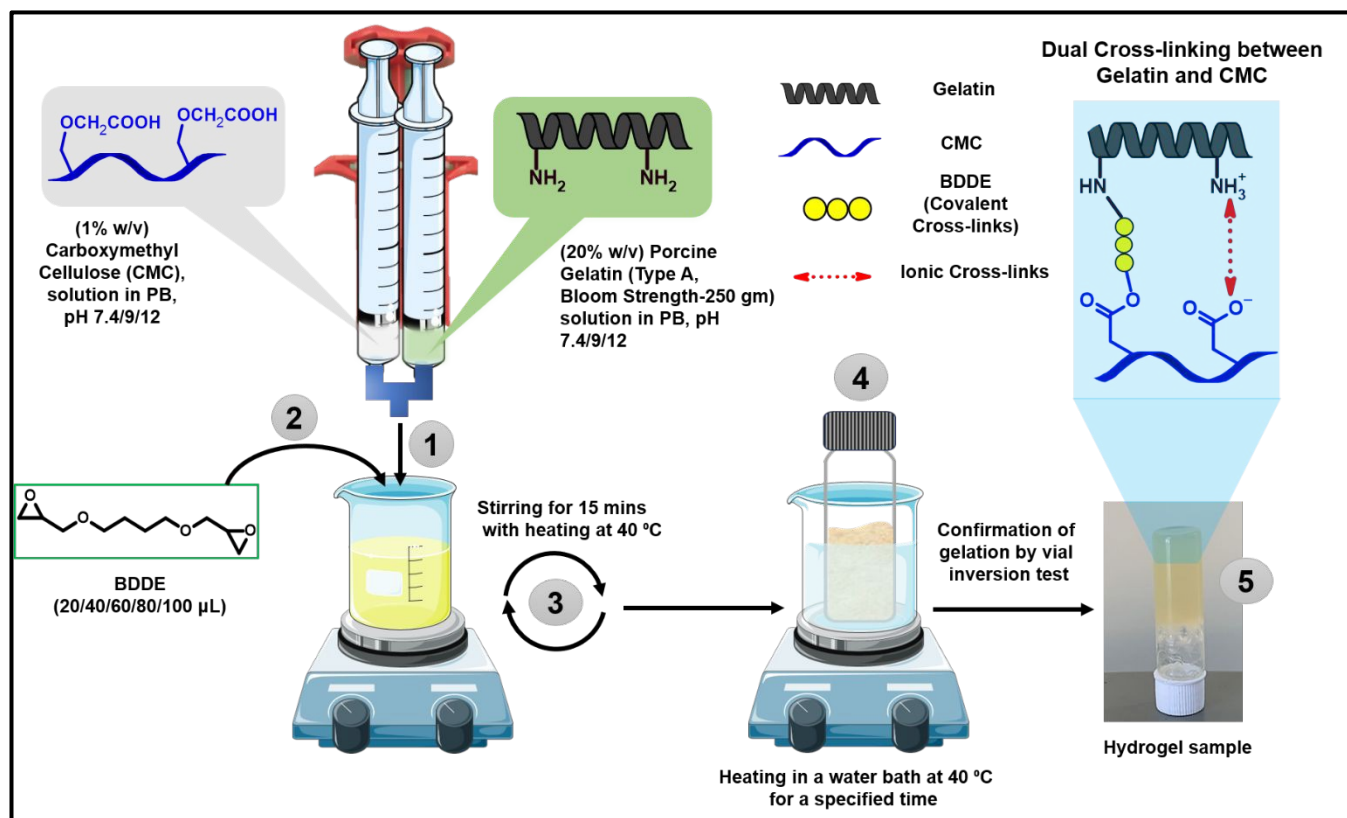


**Figure 2:** General procedure to formulate pH-responsive hydrogel.

dialdehydes, BDDE and DVS for cross-linking one type of polymer, either cationic or anionic polyelectrolytes. For example, Faivre *et al.* reviewed and reported cross-linking of hyaluronic acid by DVS and BDDE.<sup>74</sup> Sala *et al.* developed a hydrogel by cross-linking two anionic polymers, HA and CMC, using BDDE.<sup>71</sup> Similarly, cationic polymers were also cross-linked to develop hydrogels, such as Privar and co-workers developed chitosan's hydrogel by using diglycidyl ethers of glycols.<sup>75</sup> On the other hand, some scientists have explored one type of cross-linking only for developing hydrogels, either through primary alcohol (e.g. for HA)<sup>74</sup> or through primary amines (e.g. for chitosan and gelatin).<sup>76</sup> It is noteworthy that incorporating the same polymer or a similar type of polymers for constructing a biomaterial formulation may limit the inclusion of beneficial features of different polymers in a single formulation. Where most of the reported pH-responsive hydrogels were found to deliver the entrapped drugs either in a basic medium or acidic medium (e.g. unidirectional).<sup>10,77</sup> In the current manuscript, we present a single hydrogel platform to deliver the drugs in both acidic medium (e.g. in the vicinity of cancer cells)<sup>20</sup> as well as in basic medium (e.g. in the proximity of chronic wounds).<sup>78</sup>

Here, we report a polyelectrolyte-based bi-directional pH-sensitive hydrogel for controlled drug delivery applications (Figure 1). The proposed hydrogel is strategically composed of gelatin, a cationic polyelectrolyte which has primary amino groups, carboxymethyl cellulose (CMC), an anionic polyelectrolyte having carboxyl groups

and a cross-linker BDDE, which is equipped with nucleophile-sensitive two epoxy functionalities at the opposite ends of propoxybutane. Primary amino groups of gelatin not only participate in generating pH-dependent cationic charge but also serve as nucleophilic cross-linking sites to react with epoxy rings of BDDE without compromising its ability to develop pH-dependent cationic charge (viz., generation of secondary amines in cross-links). In the case of CMC, carboxyl groups participate to generate pH-dependent anionic charge and contribute as cross-linking sites to react with epoxy rings of BDDE. All three basic components, gelatin, CMC and BDDE, are USFDA approved for biomaterials and implants and are known for being biodegradable and biocompatible.<sup>79–81</sup> Thus, the significance of the formulated hydrogel lies in the following features: (I) Bi-directional pH-responsive behaviour, (II) Controlled drug release in acidic as well as basic medium, (III) Highly reversible pH-responsiveness, (IV) Biodegradability, (V) Non-toxic to mammalian cells, and (VI) Affordable and scalable formulation, an essential criterion for “bench to bedside” translation. The structural and performance details of the hydrogels prepared from these natural polyelectrolytes (NPEs) are presented below:

## 2. Experimental Section

### 2.1. Materials and Methods

Gelatin type A (bloom strength -250 gm), CMC (avg. mol wt -20 KDa)



**Table 1:** Optimisation of gelation time as a function of volume ratio of CMC, gelatin and BDDE and pH.

Types of Gel	Volume of Gelatin (mL) (20 % w/v)	Volume of CMC (mL) (1 % w/v)	Volume of BDDE ( $\mu$ L)	Volume Ratio (CMC: Gelatin: BDDE)	Gelation Time* at pH 7.4 Mean $\pm$ SD (hr) (n=3)	Gelation Time* at pH 9 Mean $\pm$ SD (hr) (n=3)	Gelation Time * at pH 12 Mean $\pm$ SD (hr) (n=3)
Gel-I	2	2	20	100: 100: 1	5.246 $\pm$ 0.18	3.176 $\pm$ 0.10	3.693 $\pm$ 0.28
Gel-II	2	2	40	50: 50: 1	5.02 $\pm$ 0.52	2.196 $\pm$ 0.14	3.873 $\pm$ 0.37
<b>Gel-III</b>	<b>2</b>	<b>2</b>	<b>60</b>	<b>33.33: 33.33 :1</b>	<b>2.683 <math>\pm</math> 0.31</b>	<b>2.183 <math>\pm</math> 0.02</b>	<b>3.133 <math>\pm</math> 0.12</b>
Gel-IV	2	2	80	25:25: 1	4.31 $\pm$ 0.12	2.223 $\pm$ 0.06	2.893 $\pm$ 0.35
Gel-V	2	2	100	20: 20: 1	4.323 $\pm$ 0.02	2.306 $\pm$ 0.06	2.643 $\pm$ 0.37

\*Gelation time was calculated by vial inversion method as per the previous reported methods.<sup>82–84</sup>

were procured from Central Drug House (P) Ltd, New Delhi, India and BDDE was procured from Spectrochem, India and Neomycin sulphate (NEO) was purchased from Yarro Chem, Mumbai, India. All the spectra were recorded using SHIMADZU UV-1800. Rheological measurements were carried out on a RheoCompas MCR302 (Anton Paar India Pvt. Ltd) rheometer. Scanning electron microscopy was performed on a high-resolution field emission scanning electron microscope JEOL JSM -7610F Plus.

## 2.2. Formulation and Optimisation of Hydrogels

20 % w/v gelatin solutions (Type A, Bloom strength 250 gm) in phosphate buffers of three different pH levels (pH 7.4, pH 9 and pH 12) were prepared by heating at 40 °C for 1 hr. Similarly, 1 % w/v CMC solutions in phosphate buffers of three different pH levels (pH 7.4, pH 9 and pH 12) were prepared at RT. 2 mL of the gelatin solution and 2 mL of CMC solution (20 % w/v) were loaded into a double-barrel syringe. The contents were co-injected into a clean vial, ensuring simultaneous mixing of both solutions (Figure 2). Subsequently, different volumes (20 $\mu$ L, 40 $\mu$ L, 60 $\mu$ L, 80 $\mu$ L and 100 $\mu$ L) of 1,4-butanediol diglycidyl ether (BDDE) were added as a crosslinking agent to the polymeric solution of all three pH levels (Table 1). Each of the solutions was stirred continuously for 15 minutes at 40 °C to ensure thorough mixing and initiation of the crosslinking reaction. After mixing, the content was transferred to vials, which were then placed in a water bath to heat the solution to 40 °C. Over time, gelation was observed, indicating the successful formation of a crosslinked hydrogel network between CMC and gelatin via BDDE (Figure 2).

## 2.3. Confirmation of Gelation-Vial Inversion Test

Gelation time for all the trials of hydrogels was determined by following the earlier published reports<sup>82–84</sup> using the vial inversion method, and are mentioned in table 1. Predetermined hydrogel solutions (Table 1) were incubated in a glass vial at a controlled temperature of 40  $\pm$  1 °C. The vials were inverted at certain time intervals to examine the flow of the hydrogel solutions by visual examination. The gelation time was identified as the point at which the hydrogel solution stopped flowing.<sup>85</sup> The gelation time of all the hydrogel samples was summarised in table 1. Among all the hydrogel samples, Gel-III (due to the shortest gelation time) was selected for further studies.

## 2.4. Swelling/Shrinking Behaviour of Hydrogel

Gel-III hydrogels were cast and cured in a cylindrical shape having a 2 cm diameter and 1 cm height. Swelling was assessed volumetrically by measuring diameter and height with a scale. Gel-III hydrogels were prepared, and the volume of the prepared hydrogels was recorded. Gel-III hydrogels were then placed separately in different beakers containing 10 mL phosphate buffer of three pH values (pH 4, pH 7.4 and pH 12) and incubated at 37  $\pm$  1 °C for a period of 1 hr. After 1 hr, gels were brought out, and then the diameter and height of the gels were measured for individual hydrogels. Volume of hydrogels (before swelling and after swelling/shrinking) was calculated by using the formula  $\pi r^2 h$ , where r and h are the radii and heights of cylindrical gels, respectively. The experiments were triplicated (n=3), and results are presented with mean values and standard deviations. The percentage of swelling/shrinking of the hydrogels is calculated by the following formula:



$$\% \text{ Swelling/Shrinking} = \frac{FV-IV}{IV} \times 100 \dots \text{Eq. 1}$$

Here;

FV= Final Volume of Hydrogels

IV= Initial Volume of Hydrogels

Positive values show swelling, and negative values indicate shrinking of hydrogels.

## 2.5. Studies of pH-Response of Hydrogel

Gel-III hydrogels were prepared and subjected to sequential immersion of the same hydrogel in buffer solutions of pH 12, pH 7.4 and pH 4 at  $37 \pm 1$  °C for 1 hr (in each buffer solution) to evaluate its pH-responsive swelling and shrinking behaviour. This sequential immersion cycle was repeated with a single gel thrice from pH 12 to pH 4 and vice-versa, keeping the mid-point pH 7.4. The volume of the hydrogel is calculated after each immersion. The experiments were triplicated (n=3), and results are presented as mean values with standard deviations.

## 2.6. Biodegradability Studies of Hydrogel

Degradation profile of prepared hydrogels was studied as per ASTM Standard, ASTM F1635 – 16 “Standard Test Method for in vitro Degradation Testing of Hydrolytically Degradable Polymer Resins and Fabricated Forms for Surgical Implants.” According to the ASTM standard, the biodegradability of hydrogel is studied by following the methods.<sup>86</sup>

### 2.6.1. By Percentage Weight Reduction

Gel-III hydrogel samples were prepared using the method described in section 2.2. These hydrogel samples were dried at 50 °C for 24 hr to get constant weights. These dried and weighed hydrogels were immersed in phosphate buffer saline (10 mL) and incubated with PBS at  $37 \pm 1$  °C. After 1, 3, 5, 7, 15 and 21 days, gels were removed from PBS and dried for 24 hrs at 50 °C to get constant weights. The % weight reduction was calculated by following the formula:

$$\text{Percentage Weight Loss} = \frac{\text{Initial Weight} - \text{Weight After Degradation}}{\text{Initial Weight}} \times 100$$

.....Eq..2

### 2.6.2. Scanning Electron Microscopy (SEM)

Scanning electron microscopy images of dried Gel-III samples were recorded to study the microscopic changes in hydrogels due to degradation. SEM images of Gel-III were recorded before degradation and of the degraded Gel-III sample after 21 days. Dried samples of Gel-III were examined by SEM (JEOL JSM -7610F Plus) after gold-coating for 60s, and images were captured at 2.00 kV acceleration voltage.

## 2.7. Rheology of Hydrogel

For studying the flow properties of the prepared hydrogels (Gel-III), rheology experiments were performed at 25 °C with a controlled stress rheometer (RheoCampass MCR302, Anton Paar) in cone plate geometry (25 mm diameter) with a 0.5 mm gap. An amplitude sweep experiment was performed from 0.1 to 1000% shear strain, and both of the moduli were recorded. Angular frequency sweep

measurements were performed from 1 to 100 rad/s (at 1% shear strain), and both of the moduli were recorded.

## 2.8. Drug Entrapment and pH-Responsive Drug Release

Neomycin sulphate (NEO) was chosen as a model drug to study pH-responsive drug release at pH 6 and pH 9. These pH values were opted for this study because of their direct correlation with diseased conditions, such as pH 6 in the proximity of cancerous cells<sup>20</sup> while chronic wounds exhibit a pH of 9.<sup>78</sup> In this regard, using NEO for this study looks relevant as neomycin sulphate is a well-known antibiotic<sup>87,88</sup> and has also been reported to show anti-cancer activity.<sup>89–91</sup>

### 2.8.1. Drug Entrapment in the Hydrogel

20% w/v and 1 % w/v solution of Gelatin (Type A, Bloom strength - 250 gm) and CMC, respectively, were prepared in phosphate buffers (PB), pH 9. 2 mL of the gelatin solution was taken out in a vial, and 100 mg of Neomycin sulphate (NEO) was dissolved in it with stirring at 40 °C. The gelatin solution containing NEO and CMC was loaded into a double-barrel syringe. The contents were co-injected into a clean beaker. Then 60 µL of BDDE was added as a crosslinking agent to the polymeric solution, ensuring proper mixing of both solutions for 15 minutes with stirring at 40 °C. After mixing, the content was transferred into a vial, which was then placed on a water bath to heat the solution at 40 °C to form the hydrogel with entrapped NEO.

### 2.8.2. Entrapment Efficiency:

Before proceeding to find out the entrapment efficacy of the hydrogel (Gel-III), it is a prerequisite to adopt a quantitative analytical method that helps to find out the drug's concentration in a solution. We opted for UV-visible spectroscopy for the same. Firstly, the solution of NEO was prepared in distilled water (5 mg/mL), and the absorption maximum was recorded as 305 nm. A series of standard solutions (1 mg/mL, 3 mg/mL, 5 mg/mL, 7 mg/mL, 9 mg/mL, and 11 mg/mL) was prepared, and the absorbance of each of the solutions was recorded at 305 nm. A standard curve was plotted between the concentration of NEO and absorbances of standard solutions of NEO to generate a straight-line equation as  $Y=0.0469X-0.0155$ , where  $Y=Abs_{305nm}$  and  $X$  is the concentration of NEO (mg/mL) (Figure S1).

Secondly, Gel-III hydrogel loaded with NEO was placed in a beaker containing 10 mL of distilled water for 2 mins to remove any surface-adsorbed NEO from the surface of the hydrogel. Sufficient aliquot was withdrawn to record the absorbance at 305 nm, and after processing through the straight-line equation, entrapment efficacy is calculated by the following formula:

$$\text{Entrapment Efficacy (\%)} = \frac{\text{Amount of NEO Loaded in Hydrogel} - \text{Adsorbed NEO on Hydrogel}}{\text{Amount of NEO Loaded in Hydrogel}} \times 100$$

.....Eq. 3



### 2.8.3. pH-Responsive Drug Release

After removing surface-adsorbed NEO from Gel-III, Gel-III was transferred to a beaker containing 10 mL of PB solution of pH 9 and allowed to soak PB for 1 hr at 37±1 °C to study the drug (NEO) release. Absorbance of the PB (containing released NEO) was measured at 305 nm. Then, the NEO-loaded Gel-III was transferred into 10 mL of PB of pH 7.4 and allowed to soak in PB for 1 hr at 37±1°C. After 1 hr, the hydrogel is removed, and the aliquot is collected to record absorbance at 305 nm. After this, the gel is transferred into 10 mL of PB pH 6 and allowed to soak in PB (pH 6) for 1 hr at 37±1 °C. The NEO-loaded gel is removed, and an aliquot is collected to record absorbance at 305 nm. Likewise, the same gel has been exposed to different pH environments (buffer solutions) (e.g. pH 7.4 → pH 9 → pH 7.4 → pH 6) for 1 hr at 37±1 °C, and after each step, absorbances of the buffer solutions were recorded at 305 nm. Thus, the obtained absorption values (which directly correlated with NEO conc.) are plotted against pH values. Additionally, the volume of the NEO-loaded Gel-III was also calculated at each step and is plotted against pH values as per the procedure mentioned in section 2.5.

### 2.9. Cytocompatibility Study (MTT Assay)

Cytocompatibility study of the prepared hydrogel is performed by MTT assay as per the previously reported method with some modifications.<sup>51</sup> In brief: hydrogel sample; Gel-III (25 µg and 50 µg) were incubated for 0, 1, 3, 5 and 7 days, in 1 mL of Dulbecco's Modified Eagle Medium (DMEM) media, supplemented with 10 % (w/v) fetal bovine (calf) serum, 100 IU/mL penicillin, 100 µg/mL streptomycin at 37 °C for extracting the degraded and leached products. HeLa cells were seeded into 96-well plates, maintained and cultured in DMEM culture medium supplemented with 10 % (w/v) fetal bovine serum, 100 IU/mL penicillin, 100 µg/mL streptomycin at 37 °C in a humidified atmosphere with 5% CO<sub>2</sub> in a CO<sub>2</sub> incubator for 24 hr (~ 1 doubling period) to form a semi-confluent monolayer; 1 × 10<sup>4</sup> cells/100 µL MEM culture medium/well. Culture medium was removed by aspiration. 100 µL of the hydrogel's extract (withdrawn from each time point) was added to the medium and incubated at 37 °C, 5% CO<sub>2</sub> for 24 hr. Cells were evaluated microscopically to observe any morphological alterations. Culture medium was removed by aspiration. 50 µL of sterilised MTT (5 mg/mL) stock solution in phosphate buffer saline (PBS) was added to each well and incubated for 3 hr. After 2 hr, the MTT solution was decanted, and formazan crystals that could be seen under the microscope were dissolved in 50 µL of DMSO. This plate was swayed and subsequently transferred to a microplate reader, and absorbance was measured at 570 nm. Absorbance is directly correlated with a higher number of viable cells. Percent cell viability can be determined by the following formula:

$$\text{Percent Cell Viability} = \frac{OD(570) \text{ Test}}{OD(570) \text{ Blank}} \times 100$$

OD (570) Test is the mean value of the measured optical density of the extracts of the hydrogel samples. OD (570) Blank is the mean value of the measured optical density of the blanks.

## 3. Results and Discussion

### 3.1. Formulation and Optimisation of Hydrogels: Insight into Internal Cross-linking

Different volume ratios of gelatin solution (20 % w/v), CMC solution (1 % w/v) and BDDE were employed at different pH 7.4, 9 and 12 to get the lowest gelation time (results are summarised in Table 1). Among all three pH values, gelation at pH 9 showed the relatively shortest gelation time at each of the BDDE concentrations. This happens because at this pH, electrostatic interactions remain optimum and suitable for dual cross-linking (Figure 1). Electrostatic interaction is the primary force to bring gelatin (positively charged polyelectrolyte) and CMC (negatively charged polyelectrolyte) into proximity. This proximity of both of the counter polyelectrolytes at this pH promotes covalent cross-linking between these oppositely charged PEs with added BDDE molecules. At pH 9, the close vicinity of primary amines of lysine groups of gelatin and carboxylate ions of CMC tends to react with epoxide rings of BDDE.<sup>92,93</sup> This was confirmed by the FTIR spectrum of the dried powder of hydrogel (GEL-III). In this spectrum (Figure S5; SI), a peak around 1779 cm<sup>-1</sup> suggests carbonyl groups in the ester groups formed by the cross-linking of -COONa of CMC with BDDE.<sup>85</sup> Peaks for secondary amines around 3300 cm<sup>-1</sup> resulted from the reaction of the primary amine of gelatin and epoxy rings of BDDE; might have merged with peaks of the other compounds (e.g. CMC) present in the xerogel (Figure S5; SI).<sup>59</sup> Hence, gelatin (cationic PE) and CMC (anionic PE) get cross-linked to generate a 3D network of hydrogel.

At pH 7.4, gelation takes more time as compared to the gelation at pH 9 and at pH 12. Although at this pH, gelatin and CMC tend to behave as cationic and anionic PEs, respectively and provide the primary force of interaction through electrostatic interaction too. Nevertheless, neutral/mild basic pH does not greatly favour primary amine (of gelatin) and BDDE reaction to cross-link with CMC.<sup>93</sup> This holds true as a larger population of primary amines of gelatin remains protonated at this pH<sup>15</sup> and have less tendency to react with BDDE.<sup>93</sup>

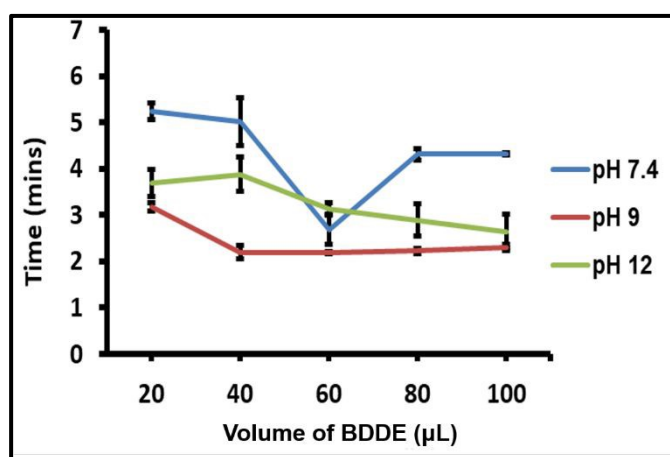


**Figure 3:** Gelation time of hydrogels as a function of pH and volume of BDDE.



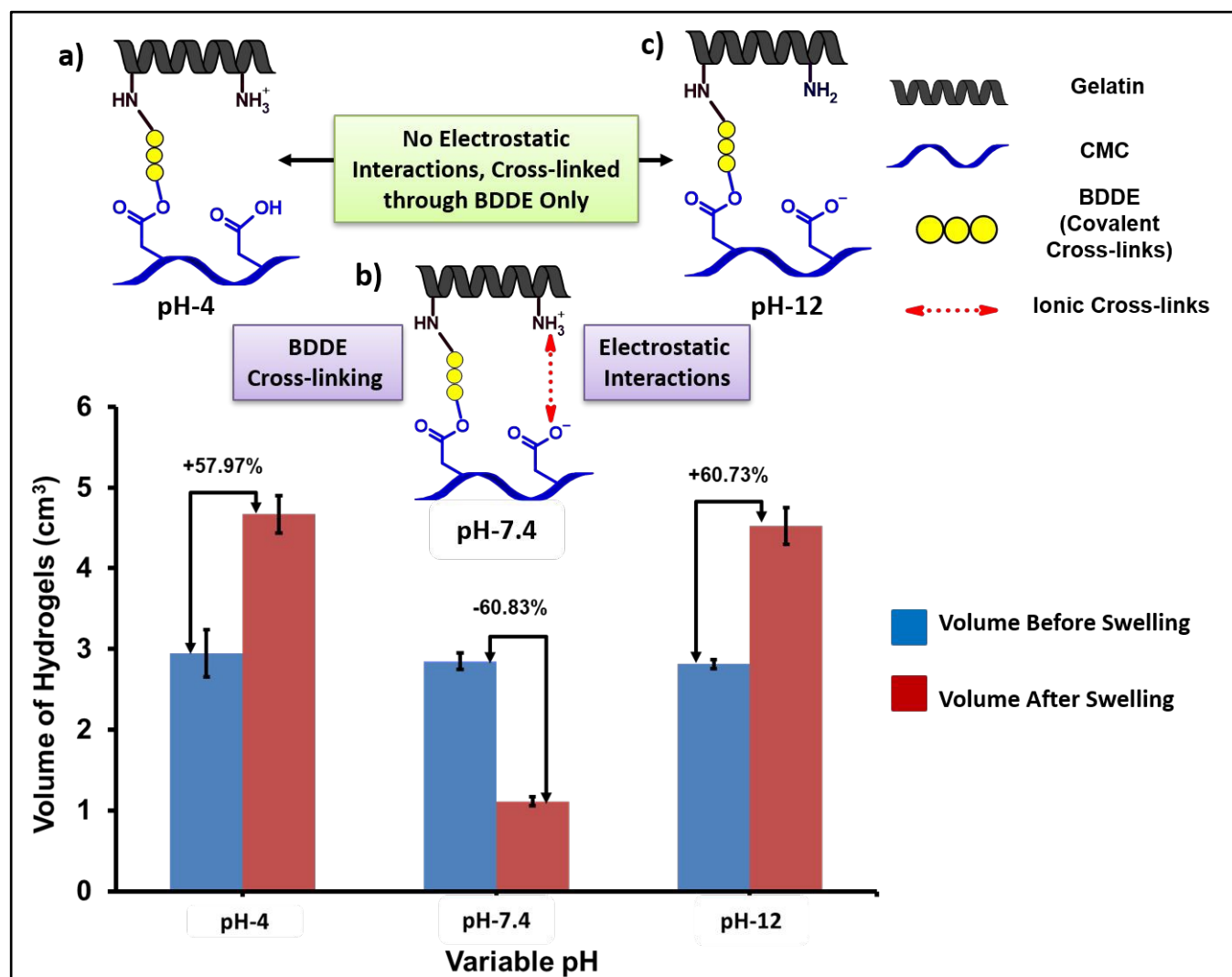


**Figure 4:** Bar graph of swelling/shrinking behaviour of the hydrogel (Gel-III) as a function of pH along with associated cross-linking; a) at pH 4 and c) at pH 12; Gel and CMC are cross-linked through BDDE only, not by ionic interactions; b) at pH 7.4; Gel and CMC are cross-linked through BDDE and ionic interactions.

However, we observed that the addition of 60  $\mu\text{L}$  of BDDE suddenly decreased the gelation time (Figure 3), which may be due to higher availability of BDDE or a higher amount of BDDE may cross-link CMC chains only.<sup>94</sup> Interestingly, further increasing BDDE amount to 80  $\mu\text{L}$  and 100  $\mu\text{L}$  may lead to an overly dense network. Excessive crosslinking can limit the mobility of polymer chains, restricting their ability to rearrange and form a gel. This can result in increased gelation time with 80 and 100  $\mu\text{L}$  of BDDE.<sup>60,95</sup>

At pH 12, gelatin type A bears a negative charge (iso-electric point of gelatin type A is 7-9); thus, it behaves as an anionic polyelectrolyte.<sup>96,97</sup> Hence, at pH 12, gelatin and CMC both behave as anionic polyelectrolytes and do not have electrostatic attraction. Lacking primary gelation force, but both of the components (gelatin

and CMC) can still undergo covalent cross-linking through BDDE with a reduced rate of reaction, which leads to a higher gelation time than gelation time at pH 9 (Figure 3).

### 3.2. Swelling/Shrinking Behaviour of Hydrogel

pH-responsive swelling and shrinking behaviour of hydrogels is a critical property that makes them a potential platform for pH-responsive drug delivery. This behaviour is governed by the interaction between the polymeric functional groups and the surrounding pH.<sup>10,98</sup> The proposed hydrogel exhibited bi-directional pH-responsive swelling. Gel-III has shown around 58 % and 61 % swelling at pH 4 and pH 12, respectively, at 37 °C within 1 hr. Contrary



to this, Gel-III showed around 61 % shrinking at pH 7.4 at 37 °C within 1 hr. (Figure 4a). Thus, the prepared hydrogel responds to pH values below and above the physiological pH 7.4, hence called a bi-directional pH-responsive hydrogel. This bi-directional pH-dependent swelling and shrinking behaviour of the prepared hydrogels is attributed to dual cross-linking of gelatin and CMC; first, one pH-dependent ionic cross-linking, while the second one is stable BDDE-based covalent cross-linking (Figures 2 and 4b). At pH 4, carboxylic groups of CMC remain protonated (-COOH);<sup>22</sup> thus, CMC does not carry a negative charge to interact with positively charged gelatin. At this pH, gelatin and CMC are connected through BDDE cross-links only. In this case, when Gel-III is immersed in the pH 4 medium, water molecules come into the hydrogel and exert osmotic pressure. This results in significant swelling of the gel, especially in the absence of electrostatic interaction between gelatin and CMC (Figure 4a). At pH 12, amine groups of gelatin remain deprotonated (uncharged) (-NH<sub>2</sub>);<sup>15</sup> thus, gelatin does not carry a positive charge to interact with negatively charged CMC. At this pH, gelatin and CMC are connected through BDDE cross-links only. In this case, when Gel-III is immersed in the pH 12 medium, water molecules come into the hydrogel and exert osmotic pressure. This results in significant swelling of the gel, especially in the absence of electrostatic interactions between gelatin and CMC (Figure 4c).

Contrary to both of the above-mentioned cases, when Gel-III is immersed in the pH 7.4 medium and allowed to reach at equilibrium at pH 7.4, amine groups of gelatin get protonated (charged) (-NH<sub>3</sub><sup>+</sup>); and carboxylic groups of CMC become deprotonated (-COO<sup>-</sup>).<sup>15,22</sup> Thus, at this pH, gelatin, which carries a positive charge, starts interacting with negatively charged CMC through ionic interactions. Restoration of electrostatic interactions between gelatin and CMC, which are already connected through BDDE cross-links, results in shrinking of Gel-III. In this case, exerted osmotic pressure is superseded by dual cross-linking; hence, we see about 61 % shrinking in Gel-III rather than swelling (Figure 4b).

### 3.3. pH-Responsiveness of Hydrogel

After studying the pH-dependent swelling/shrinking, we investigated the effect of three reversible cycles of pH change to evaluate the reversible pH responsiveness (swelling/shrinking behaviour) of a single sample of hydrogel, Gel-III. Gel-III exhibited prominent swelling after experiencing pH 12 (point B and F, Figure 5) and pH 4 (point D and H, Figure 5) environments. As discussed earlier, this happens due to compromised electrostatic bonding between gelatin and CMC at pH 12 and pH 4. Transferring the same hydrogel sample in PB pH 7.4 intermittently resulted in significant shrinking (points C, E and G, Figure 5). Thus, the produced shrinking was attributable to the restoration of electrostatic (ionic) attraction between the ammonium ions of gelatin and the carboxylate ions of CMC at pH 7.4. This experiment confirms the repetitive bi-directional pH-sensitive swelling, which strongly advocates that this same hydrogel platform may be utilised for delivering the drugs in acidic environments as well as basic media.

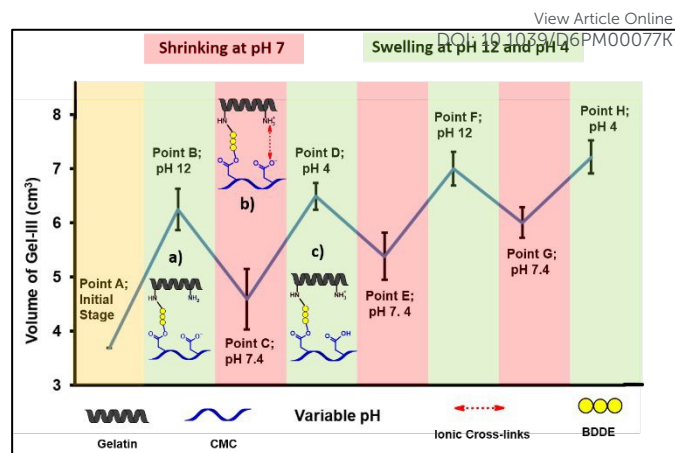


**Figure 5.** pH-induced swelling-shrinking cycle of a single Gel-III hydrogel sample. Embedded figures a), b), and c) represent types of cross-linking between gelatin and CMC, at pH 12, 7.4 and 4.

### 3.4. Rheology of Hydrogel

The rheological profile of the prepared hydrogel can be employed to evaluate the flow properties. Judicious fluidity/modulus decides the ease of handling/applicability of the hydrogel on the biological surfaces. Firstly, the fluidity of hydrogel Gel-III is evaluated by calculating storage modulus ( $G'$ ) and loss modulus ( $G''$ ) of the hydrogel by conducting an amplitude sweep experiment. The amplitude (strain) sweep experiment reflects that the prepared hydrogel (Gel-III) can stand with 0.1% to 100 % strain (upper panel; Figure 6). It suggests that the prepared hydrogel was found to be robust enough to handle during transportation and transferring from packaging to the application site.<sup>99</sup>

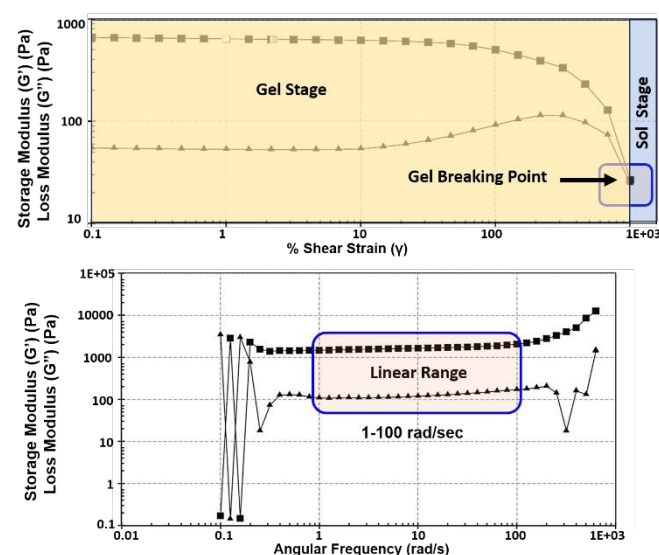


**Figure 6.** Upper panel: Amplitude (strain) sweep (from 0.1 to 1000%) rheological study of hydrogel Gel-III. Lower panel: Frequency sweep (from 0.1 to 1000 rad/sec frequency) rheological study of hydrogel Gel-III at 1% strain.



Storage modulus of the gel remains higher than loss modulus before the gel breaking point at 1000% strain. Secondly, the frequency sweep experiment shows that the  $G'$  value was higher than the  $G''$  value from 1 to 100 rad/sec frequency range (lower panel; Figure 6). These results confirm the gel-like character of the prepared hydrogel over the frequency range (1-100 rad/sec) and indicate that the hydrogel maintains its internal structure under substantial applied strain.

### 3.5. Biodegradability Studies

Biodegradability of the prepared hydrogel is a crucial attribute for biomedical applications. We found that Gel-III underwent 90% weight reduction in 21 days in phosphate buffer pH 7.4 at 37°C (Figure 7). This degradation profile looks promising for wound healing applications due to similar time points involved for wound/skin repair and the hydrogel's degradation.<sup>100</sup> The degradation of the hydrogel (Gel-III) was further assured at the microscopic level, also by SEM studies before and after degradation (Figure 7; inset images). The captured SEM micrographs confirm the surface erosion through the formation of fluffy and expanded bulges during the degradation of the hydrogels.

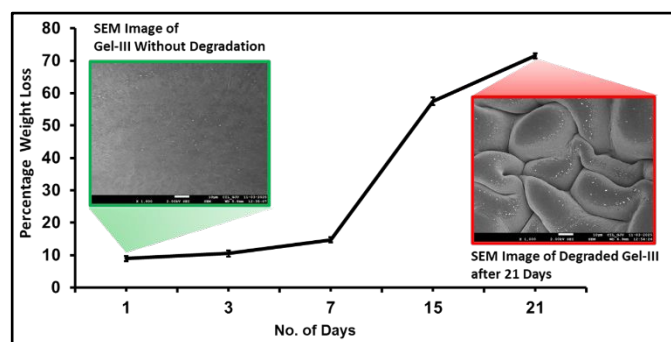


**Figure 7.** Degradation profile of hydrogel (Gel-III) obtained by percentage weight reduction method according to ASTM F1635-16 protocol and by observing corresponding SEM macroscopic images (inset images). Surface bulging was observed in SEM micrographs of the degraded hydrogel (Gel-III).

### 3.6. Scanning Electron Microscopy (SEM) of Prepared Hydrogel

SEM micrographs of Gel-III hydrogel were recorded before degradation and after 21 days (after ~90% degradation) to study the effect of degradation on the morphology of hydrogel samples. SEM micrograph of an intact (before degradation) hydrogel sample shows comparatively smooth (no fluffy bulges) surface, even at 5000 x magnification (Figure 8a; inset image), while the degraded hydrogel sample shows fluffy bulges pointing towards outside (Figure 8b; yellow arrow and lines), which may be due to the stretched hydrogel surface because of osmotic pressure; hydrogel faced during the degradation. These results are consistent with earlier published reports regarding hydrogels' swelling and degradation.<sup>100-102</sup>

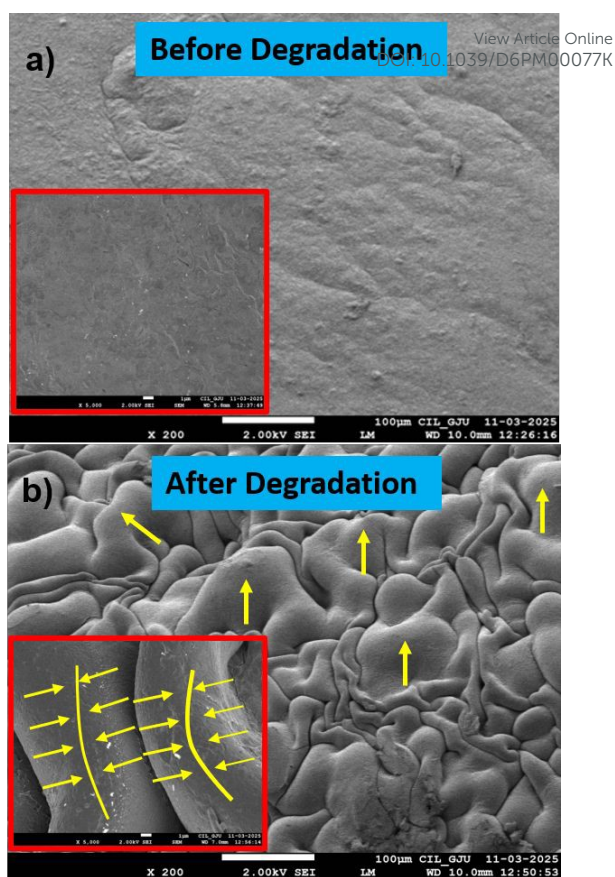


**Figure 8.** Representative SEM micrographs of a) hydrogel sample Gel-III before degradation, showing a flat surface; and b) after 21 days of degradation, showing multiple bulges on the surface of the hydrogel. Images in insets (in red rectangles) are magnified images of the respective micrographs. The yellow arrow and lines are showing prominent bulges due to degradation.

### 3.7. Drug and Entrapment and Release

We then probed the applicability of this hydrogel towards a bi-directional pH-responsive drug delivery application. For this exploration, we selected two pH values, pH 6 and pH 9 (below and above physiological pH, respectively) for pH-responsive drug release because the vicinity of tumour cells has a pH around 6, while basic pH 9 prevails in the proximity of chronic wounds.<sup>20,78</sup> The prepared gel, Gel-III, could efficiently incorporate the antibiotic drug neomycin sulphate (NEO), which additionally has shown some anti-cancer effect.<sup>89-91</sup> NEO could be entrapped with 84 % efficiency. This excellent entrapment efficiency is attributed to ionic interactions between the ammonium groups ( $\text{NH}_3^+$ ) of NEO and the carboxylate groups ( $\text{COO}^-$ ) of CMC at physiological pH (7.4). These ionic interactions prevail around pH 7.4 but become weaker at pH 9 and 6. This happens because, as compared to pH 7.4, a lower proportion of primary amines remains protonated (positively charged) at pH 9, while a lower proportion of carboxylate anion is available at pH 6. This reduced ionic interactions between NEO and CMC at pH 6 and 9 contribute to the release of NEO from the hydrogel.



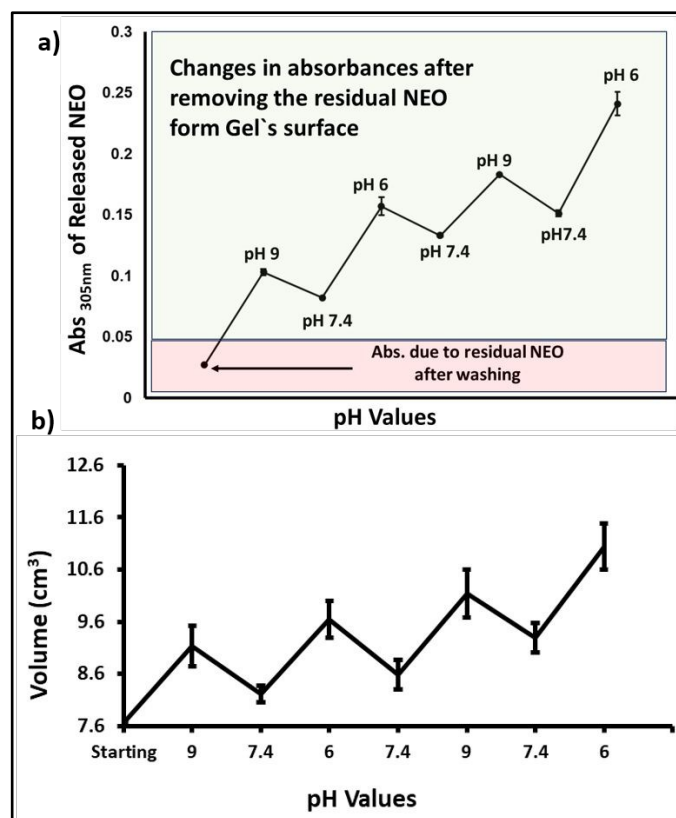


**Figure 9.** a) Repeated pH-responsive release of neomycin sulphate (NEO); b) analogous pH-responsive swelling and shrinking behaviour of hydrogel sample Gel-III.

This hypothesis is nicely reflected in the changes in absorbance values (at 305 nm) of released NEO at pH 6 and pH 9 as compared to the absorbance values at pH 7.4 (Figure 9a). This trend strongly advocates that entrapped NEO can be released prominently in PB of pH 6 and pH 9 as compared to pH 7.4. This release profile follows the swelling and shrinking behaviour of hydrogel, where pH 6 and pH 9 exhibit swelling and pH 7.4 results in the shrinking of the hydrogel (Figure 9b). Following the discussion in section 3.3, at pH 7.4, electrostatic interactions between gelatin and CMC remain prominent as compared to at pH 6 and pH 9 (BDDE cross-links remain constant for all three pH). At pH 6 and pH 9, lower ionic interactions between gelatin and CMC allow the hydrogel to swell due to osmotic pressure. This swelling, along with the subdued ionic interactions with NEO and CMC, resulted in higher release of NEO at both of the pH values. On the other hand, at pH 7.4, superior electrostatic interactions between gelatin and CMC force the hydrogel to shrink. In addition to the shrinkage of the hydrogel at pH 7.4, strong ionic interactions between NEO and CMC at this pH value restrict the drug release, which is reflected by lower absorbance values at 305 nm. A few controversial and divergent hypotheses about drug release, such as degradation-induced release and diffusion-induced release, can be ruled out in this case.<sup>103</sup> In the first case, entrapped drug NEO is released as a function of pH only within a daytime where degradation of the hydrogel is negligible, while in the second case, NEO can be released after charged neutralisation (either CMC or on NEO) and osmotic pressure, not by diffusion only. Thus, observations of these

experiments strongly suggest the potential of the prepared hydrogels for bi-directional, on-demand pH-responsive drug delivery at both of the clinically relevant pH values.

### 3.8. Cytocompatibility Studies

The prepared hydrogel sample (Gel-III) was found to show around 100% cell viability for HeLa cell lines up to 7 days at 25 µg/mL and 50 µg/mL (Figure 10). These results reconfirm the biocompatibility of gelatin, CMC and BDDE.<sup>59,104,105</sup>

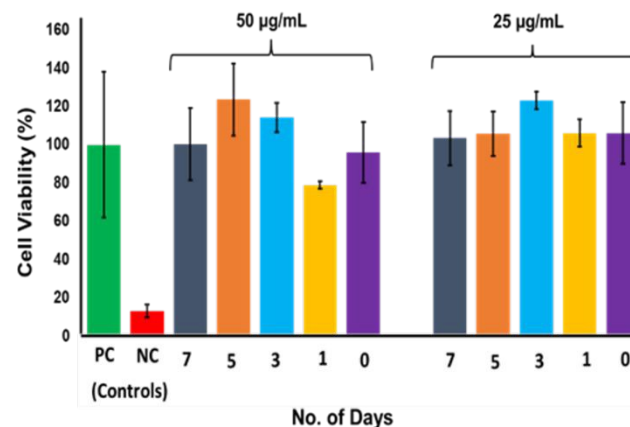


**Figure 10.** Percentage cell viability of the hydrogel sample Gel-III after different days of incubation with HeLa Cells. HeLa cells, along with media without any hydrogel sample, were taken as a positive control, and Triton X-100 was taken as a negative control.

### 4. Conclusion

In conclusion, we have demonstrated the development of a bi-directional pH-responsive hydrogel platform for drug delivery. These hydrogels are fabricated from oppositely charged polyelectrolytes and have dual cross-linking; one is pH-dependent ionic cross-linking, while the other is BDDE-based covalent cross-linking. These hydrogels reversibly respond to both acidic and basic pH and deliver the entrapped drug effectively. The hydrogels are biodegradable, and all their components are FDA approved. Optimisation of BDDE content in the hydrogel Gel-III afforded the shortest gelation time. The hydrogel degraded on its own in about three weeks. The drug-delivery potential of this hydrogel was shown by the pH-assisted release of entrapped neomycin sulphate in acidic and as well as in basic pH. The formulation of this pH-responsive hydrogel system does not require any special equipment and is free from organic solvents. All the components (gelatin, CMC and BDDE) of the proposed hydrogel system are cost-effective. Although this hydrogel system may face some limitations, such as it can be used efficiently for a shorter period of time only, due to its 90% degradation occurring within 21 days. Another minor challenge it may face is the requirement of the fabrication of a larger double-barrel container with suitable mixers to mix CMC and gelatin. Considering all the pros and cons, we believe that the proposed hydrogel is suitable for scaling up.



## 5. Acknowledgements

The authors are thankful to GD Goenka University, Sohna, for infrastructure support. Authors are thankful to Dr. Rajendra Kurapati, Indian Institute of Science Education and Research, Thiruvananthapuram, for conducting cell cytotoxicity studies in his lab.

## 6. Declarations

**Conflict of interest:** The authors declare that they have no conflicts of interest.

**7. Funding:** There is no funding for the research mentioned in this manuscript.

**8. Supporting Information:** Supporting information includes a standard curve of neomycin sulphate (NEO) in water. FTIR spectrum of gelatin, CMC, BDDE and dried hydrogel formulation Gel-III.

## 9. References:

- J. Li and D. J. Mooney, *Nat. Rev. Mater.*, 2016, **1**, 1–17.
- R. Narayanaswamy and V. P. Torchilin, *Molecules*, 2019, **24**, 603.
- S. J. Buwalda, T. Vermonden and W. E. Hennink, *Biomacromolecules*, 2017, **18**, 316–330.
- M. Rizwan, R. Yahya, A. Hassan, M. Yar, A. Azzahari, V. Selvanathan, F. Sonsudin and C. Abouloula, *Polymers (Basel)*, 2017, **9**, 137.
- A. Bordbar-Khiabani and M. Gasik, *Int. J. Mol. Sci.*, 2022, **23**, 3665.
- Y. Li, X. Ding, H. Hu and F.-J. Xu, *Precision Medicine and Engineering*, 2024, **1**, 100001.
- A. Alsuraifi, A. Curtis, D. A. Lamprou and C. Hoskins, *Pharmaceutics*, 2018, **10**, 136.
- L. P. Tricou, M. L. Al-Hawat, K. Cherifi, G. Manrique, B. R. Freedman and S. Matoori, *Adv. Wound Care (New Rochelle)*, 2024, **13**, 446–462.
- Y. Liu, W. Kang, L. Nie, F. Xiao, Y. Li, Q. Ma, D. Lin, G. Zhou, S. Liu, K. Sun and X. Li, *React. Funct. Polym.*, 2024, **204**, 106025.
- P. Gupta, K. Vermani and S. Garg, *Eur. J. Pharm. Sci.*, 2002, **15**, 187–192.
- G. Kocak, C. Tuncer and V. Bütün, *Polym. Chem.*, 2017, **8**, 144–176.
- K. Lavanya, S. V. Chandran, K. Balagangadharan and N. Selvamurugan, *Mater. Sci. Eng., C*, 2020, **106**, 110862. [View Article Online](#) DOI: 10.1016/j.mse.2020.110862
- Y. Che, D. Li, Y. Liu, Q. Ma, Y. Tan, Q. Yue and F. Meng, *RSC Adv.*, 2016, **6**, 106648–106655.
- M. Mahdian, S. Akbari Asrari, M. Ahmadi, T. Madrakian, N. Rezvani Jalal, A. Afkhami, M. Moradi and L. Gholami, *J. Drug Deliv. Sci. Technol.*, 2023, **84**, 104537.
- Z. Cimen, S. Babadag, S. Odabas, S. Altuntas, G. Demirel and G. B. Demirel, *ACS Appl. Polym. Mater.*, 2021, **3**, 3504–3518.
- S. Bahmani, R. Khajavi, M. Ehsani, M. K. Rahimi and M. R. Kalaei, *Int. J. Biol. Macromol.*, 2025, **284**, 138034.
- X. Shi, M. Lan, J. Liu, J. Zhou and H. Gu, *Polymer (Guildf)*, 2024, **308**, 127365.
- S. Setoyama, R. Haraguchi, S. Aoki, Y. Oishi and T. Narita, *Int. J. Mol. Sci.*, 2024, **25**, 10439.
- J. Yang, Z. Zhu, J. Zhang, C. Chen, Z. Lei, L. Li, Z. Feng and X. Su, *J. Polym. Res.*, 2023, **30**, 1–9.
- Y. Wu, Y. Li, R. Han, Z. Long, P. Si and D. Zhang, *Biomacromolecules*, 2023, **24**, 5364–5370.
- T. Thambi, J. M. Jung and D. S. Lee, *Biomater. Sci.*, 2023, **11**, 1948–1961.
- R. R. Mohamed, M. E. Fahim and S. M. A. Soliman, *BMC Chem.*, 2022, **16**, 1–12.
- D. S. Lima, E. T. Tenório-Neto, M. K. Lima-Tenório, M. R. Guilherme, D. B. Scariot, C. V. Nakamura, E. C. Muniz and A. F. Rubira, *J. Mol. Liq.*, 2018, **262**, 29–36.
- T. S. Anirudhan, M. Mohan and M. R. Rajeev, *Int. J. Biol. Macromol.*, 2022, **201**, 378–388.
- H. Suo, M. Hussain, H. Wang, N. Zhou, J. Tao, H. Jiang and J. Zhu, *Biomacromolecules*, 2021, **22**, 3049–3059.
- A. R. Simão, V. H. Fragal, A. M. de O. Lima, M. C. G. Pellá, F. P. Garcia, C. V. Nakamura, E. B. Tambourgi and A. F. Rubira, *Int. J. Biol. Macromol.*, 2020, **148**, 302–315.
- C. Chang, M. He, J. Zhou and L. Zhang, *Macromolecules*, 2011, **44**, 1642–1648.
- S. H. Park, H. S. Shin and S. N. Park, *Carbohydr. Polym.*, 2018, **200**, 341–352.
- J. S. Vuković, M. Žabčić, L. Gazvoda, M. Vukomanović, T. R. Ilić-Tomić, D. R. Milivojević and S. L. Tomić, *Biopolymers*, 2025, **116**, e70008.



## ARTICLE

## Journal Name

- 30 P. S. Yavvari, A. K. Awasthi, A. Sharma, A. Bajaj and A. Srivastava, *J. Mater. Chem. B*, 2019, **7**, 2102–2122. 49 J. R. Clegg, K. Adebawale, Z. Zhao and S. Mitragotri, *Bioeng. Transl. Med.*, 2024, **9**, e10680. DOI: 10.1039/D6PM00077K
- 31 B. Benj, B. Gyarmati, Árpád, A. Árpád, N. Emethy, A. Andr and A. Szii, *RSC Adv.*, 2014, **4**, 8764–8771. 50 M. Ahangarpour, I. Kavianinia and M. A. Brimble, *Org. Biomol. Chem.*, 2023, **21**, 3057–3072.
- 32 S. Nesrinne and A. Djamel, *Arab. J. Chem.*, 2017, **10**, 539–547. 51 T. N. Pham, C. F. Su, C. C. Huang and J. S. Jan, *Colloids Surf. B Biointerfaces*, 2020, **196**, 111316.
- 33 X. Gao, C. He, C. Xiao, X. Zhuang and X. Chen, *Polymer (Guildf)*, 2013, **54**, 1786–1793. 52 B. Liu, L. Burdine and T. Kodadek, *J. Am. Chem. Soc.*, 2006, **128**, 15228–15235.
- 34 R. Pappalardo, M. Boffito, C. Cassino, V. Caccamo, V. Chiono and G. Ciardelli, *ACS Omega*, 2024, **9**, 25609–25621. 53 M. Krogsgaard, M. A. Behrens, J. S. Pedersen and H. Birkedal, *Biomacromolecules*, 2013, **14**, 297–301.
- 35 F. Hakimi, L. Maeso, A. Dehghan, A. Dolatshahi-Pirouz, Goran, M. Stojanovic, M. Nadimifar, Z. Ahmadian and G. Orive, *ChemistrySelect*, 2025, **10**, e05175. 54 J. W. Bae, J. H. Choi, Y. Lee and K. D. Park, *J. Tissue Eng. Regen. Med.*, 2015, **9**, 1225–1232.
- 36 S. Li, M. Pei, T. Wan, H. Yang, S. Gu, Y. Tao, X. Liu, Y. Zhou, W. Xu and P. Xiao, *Carbohydr. Polym.*, 2020, **250**, 116922. 55 G. Yang, Z. Xiao, X. Ren, H. Long, H. Qian, K. Ma and Y. Guo, *PeerJ*, 2016, **2016**, e2497.
- 37 H. Su, R. Zheng, L. Jiang, N. Zeng, K. Yu, Y. Zhi and S. Shan, *Carbohydr. Polym.*, 2021, **265**, 118085. 56 A. Sharma, S. Kundu, A. Reddy M, A. Bajaj and A. Srivastava, *Macromol. Biosci.*, 2013, **13**, 927–937.
- 38 V. T. Tran, M. T. I. Mredha, J. Y. Na, J. K. Seon, J. Cui and I. Jeon, *Chemical Engineering Journal*, 2020, **394**, 124941. 57 A. Sharma, T. Dutta and A. Srivastava, *Chemistry – A European Journal*, 2024, **30**, e202302157.
- 39 K. Yang, K. Wei, M. de Lapeyrière, K. Maniura-Weber and M. Rottmar, *Cell Rep. Phys. Sci.*, 2024, **5**, 101809. 58 G. Mugnaini, R. Gelli, L. Mori and M. Bonini, *ACS Appl. Polym. Mater.*, 2023, **5**, 9192–9202.
- 40 H. Ding, B. Li, Y. Jiang, G. Liu, S. Pu, Y. Feng, D. Jia and Y. Zhou, *Carbohydr. Polym.*, 2021, **251**, 117101. 59 K. De Bouille, R. Glogau, T. Kono, M. Nathan, A. Tezel, J. X. Roca-Martinez, S. Paliwal and D. Stroumpoulis, *Dermatologic Surgery*, 2013, **39**, 1758–1766.
- 41 S. Summonte, G. F. Racaniello, A. Lopodota, N. Denora and A. Bernkop-Schnürch, *J. Control. Release*, 2021, **330**, 470–482. 60 J. A. Del Olmo, L. Pérez-álvarez, V. S. Martínez, S. B. Cid, R. P. González, J. L. Vilas-Vilela and J. M. Alonso, *Gels*, 2022, **8**, 223.
- 42 L. J. Macdougall, M. M. Pérez-Madrugal, M. C. Arno and A. P. Dove, *Biomacromolecules*, 2018, **19**, 1378–1388. 61 G. Martínez-Mejía, N. A. Vázquez-Torres, A. Castell-Rodríguez, J. M. del Río, M. Corea and R. Jiménez-Juárez, *Colloids Surf. A Physicochem. Eng. Asp.*, 2019, **579**, 123658.
- 43 S. Yigit, R. Sanyal and A. Sanyal, *Chem. Asian J.*, 2011, **6**, 2648–2659. 62 I. H. Yang, I. E. Lin, T. C. Chen, Z. Y. Chen, C. Y. Kuan, J. N. Lin, Y. C. Chou and F. H. Lin, *Carbohydr. Polym.*, 2021, **260**, 117832.
- 44 T. M. FitzSimons, E. V. Anslyn and A. M. Rosales, *ACS Polymers Au*, 2021, **2**, 129–136. 63 B. B. Pinheiro, N. S. Rios, E. Rodríguez Aguado, R. Fernandez-Lafuente, T. M. Freire, P. B. A. Fechine, J. C. S. dos Santos and L. R. B. Gonçalves, *Int. J. Biol. Macromol.*, 2019, **130**, 798–809.
- 45 A. Andersen, M. Krogsgaard and H. Birkedal, *Biomacromolecules*, 2018, **19**, 1402–1409. 64 J. R. Dias, S. Baptista-Silva, C. M. T. de Oliveira, A. Sousa, A. L. Oliveira, P. J. Bártolo and P. L. Granja, *Eur. Polym. J.*, 2017, **95**, 161–173.
- 46 F. Lee, K. H. Bae and M. Kurisawa, *Biomed. Mater.*, 2016, **11**, 014101. 65 M. Chauhan, P. Roopmani, J. Rajendran, K. P. Narayan and J. Giri, *Int. J. Biol. Macromol.*, 2025, **285**, 138200.
- 47 H. Pan, Y. Qu, F. Wang, S. Zhao and G. Chen, *Colloid Interface Sci. Commun.*, 2025, **66**, 100828.
- 48 R. Wakabayashi, W. Ramadhan, K. Moriyama, M. Goto and N. Kamiya, *Polym. J.*, 2020, **52**, 899–911.



- | Journal Name   | ARTICLE  |
|--|--|
| 66 X. Li, W. Xue, C. Zhu, D. Fan, Y. Liu and M. Xiaoxuan, <i>Mater. Sci. Eng., C</i> , 2015, <b>57</b> , 189–196.  | 83 H. Ren, Z. Zhang, X. Cheng, Z. Zou, X. Chen and C. He, <i>Sci. Adv.</i> , 2024, <b>10</b> , eadh4327. DOI: 10.1039/D6PM00077K                                       |
| 67 X. Wu, L. Black, G. Santacana-Laffitte and C. W. Patrick, <i>J. Biomed. Mater. Res. A</i> , 2007, <b>81</b> , 59–65.  | 84 X. Xue, K. Liang, W. Huang, H. Yang, L. Jiang, Q. Jiang, T. Jiang, B. Lin, Y. Chen, B. Jiang and S. Komarneni, <i>Macromolecules</i> , 2022, <b>55</b> , 6474–6486. |
| 68 J. She, J. Liu, Y. Mu, S. Lv, J. Tong, L. Liu, T. He, J. Wang and D. Wei, <i>React. Funct. Polym.</i> , 2025, <b>207</b> , 106136.  | 85 Z. Huang, X. Xiao, X. Jiang, S. Yang, C. Niu, Y. Yang, L. Yang, C. Li and L. Feng, <i>Polym. Test.</i> , 2023, <b>119</b> , 107936.                                 |
| 69 S. Khunmanee, Y. Jeong and H. Park, <i>J. Tissue Eng.</i> , 2017, <b>8</b> , 2041731417726464.  | 86 L. N. Woodard and M. A. Grunlan, <i>ACS Macro Lett.</i> , 2018, <b>7</b> , 976–982.   |
| 70 G. Buhus, M. Popa and J. Desbrieres, <i>J. Bioact. Compat. Polym.</i> , 2009, <b>24</b> , 525–545.  | 87 B. S. Alotaibi, A. K. Khan, M. Ijaz, H. Yasin, S. Nawazish, S. Sadiq, S. Kaleem and G. Murtaza, <i>ACS Omega</i> , 2023, <b>8</b> , 39014–39022.                    |
| 71 D. Sala, F. ; Di Gennaro, M. ; Makvandi, P. ; Borzacchiello, W. Ji, F. Della Sala, M. Di Gennaro, P. Makvandi and A. Borzacchiello, <i>Gels</i> 2024, Vol. 10, Page 67, 2024, <b>10</b> , 67. | 88 Y. Li, Y. Yao, Y. Wang, Y. Lin, Y. He, S. Gao and X. Cai, <i>Nanoscale</i> , 2025, <b>17</b> , 15356–15365.   |
| 72 A. Sannino, M. Madaghiele, F. Conversano, G. Mele, A. Maffezzoli, P. A. Netti, L. Ambrosio and L. Nicolais, <i>Biomacromolecules</i> , 2004, <b>5</b> , 92–96.                                | 89 G. F. Hu, <i>Proc. Natl. Acad. Sci. U. S. A.</i> , 1998, <b>95</b> , 9791–9795.   |
| 73 V. M. de Oliveira Cardoso, B. Stringhetti Ferreira Cury, R. C. Evangelista and M. P. Daflon Gremião, <i>J. Mech. Behav. Biomed. Mater.</i> , 2017, <b>65</b> , 317–333.                       | 90 P. Cuevas, D. Díaz-González and M. Dujovny, <i>Neurol. Res.</i> , 2003, <b>25</b> , 691–693.  |
| 74 J. Faivre, A. I. Pigweh, J. Iehl, P. Maffert, P. Goekjian and F. Bourdon, <i>Expert Rev. Med. Devices</i> , 2021, <b>18</b> , 1175–1187.  | 91 P. Cuevas, D. Diaz-González, F. Carceller and M. Dujovny, <i>Neurol. Res.</i> , 2003, <b>25</b> , 13–16.  |
| 75 Y. Privar, A. Skatova, M. Maiorova, A. Golikov, A. Boroda and S. Bratskaya, <i>Gels</i> , 2024, <b>10</b> , 483.  | 92 L. A. Tziveleka, A. Sapalidis, S. Kikionis, E. Aggelidou, E. Demiri, A. Kritis, E. Ioannou and V. Roussis, <i>Materials</i> , 2020, <b>13</b> , 1763.               |
| 76 Z. Peng, Z. Peng and Y. Shen, <i>Polym. Plast. Technol. Eng.</i> , 2011, <b>50</b> , 1160–1164.   | 93 O. S. Lawal, M. Yoshimura, R. Fukae and K. Nishinari, <i>Colloid Polym. Sci.</i> , 2011, <b>289</b> , 1261–1272.  |
| 77 G. Patroklou, E. Triantafyllopoulou, P. E. Goula, V. Karali, M. Chountoulesi, G. Valsami, S. Pispas and N. Pippa, <i>Polymers (Basel)</i> , 2025, <b>17</b> , 1451.                           | 94 S. C. Choi, M. A. Yoo, S. Y. Lee, H. J. Lee, D. H. Son, J. Jung, I. Noh and C. W. Kim, <i>J. Biomed. Mater. Res. A</i> , 2015, <b>103</b> , 3072–3080.              |
| 78 L. P. Tricou, M. L. Al-Hawat, K. Cherifi, G. Manrique, B. R. Freedman and S. Matoori, <i>Adv. Wound Care (New Rochelle)</i> , 2024, <b>13</b> , 446–462.                                      | 95 Y. Tan, Y. Zi, J. Peng, C. Shi, Y. Zheng and J. Zhong, <i>Food Chem.</i> , 2023, <b>423</b> , 136265.   |
| 79 F. Della Sala, M. di Gennaro, P. Makvandi and A. Borzacchiello, <i>Gels</i> , 2024, <b>10</b> , 67.   | 96 K. J. Goudie, S. J. McCreath, J. A. Parkinson, C. M. Davidson and J. J. Liggat, <i>J. Polym. Sci.</i> , 2023, <b>61</b> , 2316–2332.                                |
| 80 M. Wojtkiewicz, A. Stachura, B. Roszkowski, N. Winiarska, K. Kazimierska and K. Stachura, <i>Aesthetic Plast. Surg.</i> , 2024, <b>48</b> , 5147–5154.  | 97 M. C. Koetting, J. T. Peters, S. D. Steichen and N. A. Peppas, <i>Mater. Sci. Eng. R Rep.</i> , 2015, <b>93</b> , 1.  |
| 81 A. Ahmady and N. H. Abu Samah, <i>Int. J. Pharm.</i> , 2021, <b>608</b> , 121037.   | 98 G. Stojkov, Z. Niyazov, F. Picchioni and R. K. Bose, <i>Gels</i> , 2021, <b>7</b> , 255.  |
| 82 S. C. Karunakaran, B. J. Cafferty, K. S. Jain, G. B. Schuster and N. V. Hud, <i>ACS Omega</i> , 2020, <b>5</b> , 344–349.   | 99 W. Zhang, L. Liu, H. Cheng, J. Zhu, X. Li, S. Ye and X. Li, <i>Mater. Adv.</i> , 2024, <b>5</b> , 1364–1394.  |
|  | 100 V. Dhote, S. Skaalure, U. Akalp, J. Roberts, S. J. Bryant and F. J. Vernerey, <i>J. Mech. Behav. Biomed. Mater.</i> , 2012, <b>19</b> , 61.                        |



## ARTICLE

## Journal Name

- 101 B. G. Stubbe, K. Braeckmans, F. Horkay, W. E. Hennink, S. C. De Smedt and J. Demeester, *Macromolecules*, 2002, **35**, 2501–2505.
- 102 Q. Xing, K. Yates, C. Vogt, Z. Qian, M. C. Frost and F. Zhao, *Sci. Rep.*, 2014, **4**, 1–10.
- 103 M. R. Bayat and M. Baghani, *J. Intell. Mater. Syst. Struct.*, 2021, **32**, 2349–2365.
- 104 A. B. Bello, D. Kim, D. Kim, H. Park and S. H. Lee, *Tissue Eng. Part B Rev.*, 2020, **26**, 164–180.
- 105 V. Tyagi and A. Thakur, *Results in Materials*, 2023, **20**, 100481.

View Article Online  
DOI: 10.1039/D6PM00077K



## Data Availability Statement

View Article Online  
DOI: 10.1039/D6PM00077K

The data supporting this article have been included as part of the Supplementary Information. Supplementary information: includes standard curve of neomycin sulphate (NEO) in water. Tables S1, S2, and S3. FTIR spectrum of gelatin, CMC, BDDE and dried hydrogel formulation Gel-III.

